

Photophysics of charge-transfer excitons in thin films of π -conjugated polymers

Zhendong Wang,¹ Sumit Mazumdar,¹ and Alok Shukla²

¹*Department of Physics, University of Arizona Tucson, AZ 85721*

²*Physics Department, Indian Institute of Technology, Powai, Mumbai 400076, India*

(Dated: November 29, 2018)

We develop a theory of the electronic structure and photophysics of interacting chains of π -conjugated polymers to understand the differences between solutions and films. While photoexcitation generates only the intrachain exciton in solutions, the optical exciton as well as weakly allowed charge-transfer excitons are generated in films. We extend existing theories of the lowest polaron-pair and charge-transfer excitons to obtain descriptions of the excited states of these interchain species, and show that a significant fraction of ultrafast photoinduced absorptions in films originate from the lowest charge-transfer exciton. Our proposed mechanism explains the simultaneous observation of polaronlike induced absorption features peculiar to films in ultrafast spectroscopy and the absence of mobile charge carriers as deduced from other experiments. We also show that there is a 1:1 correspondence between the essential states that describe the photophysics of single chains and of interacting chains that constitute thin films.

PACS numbers: 42.70.Jk, 71.35.-y, 78.20.Bh, 78.30.Jw

I. INTRODUCTION

The photophysics of dilute solutions and thin films of π -conjugated polymers (PCPs) are often remarkably different^{1,2,3,4,5,6,7,8,9,10,11,12,13,14,15,16,17,18,19}. It is generally accepted that solutions exhibit behavior characteristic of single strands, and the different behavior of films is due to interchain interaction and disorder. Microscopic understanding of the effects of interchain interaction has remained incomplete even after intensive investigations. As discussed below, to a large extent this is because the experimental results themselves, or their interpretations are controversial and confusing. Theoretical investigations of the effects of interchain interactions^{17,20,21,22,23,24,25,26,27,28} have until now focused largely on the lowest interchain species near the optical edge, and the role of such interchain species on the emissive behavior of films. The goal of this work is to re-examine interchain interaction in PCPs within a semi-empirical Hamiltonian with realistic parameters, focusing on ultrafast photoinduced absorption (PA) measurements and related experimental results that appear to be mutually contradictory. We show that theoretical understanding of *excited states* of interchain species is crucial for this purpose.

The interchain species we will be interested in have been discussed by numerous authors over the years, and the nomenclature has sometimes been confusing. It is therefore important to fix the nomenclature before we begin. We will refer to intrachain neutral excitations as *excitons*, independent of their binding energy. At the other extreme are the *polaron-pairs*, which consist of two *completely ionic charged chains*, one positive and one negative. Since we consider nonzero interchain Coulomb interactions, and since we will be discussing two-chain systems only, the polaron-pair states are necessarily bound by Coulomb interactions. For nonzero electron hopping between the chains, eigenstates that are superpositions

of the intrachain exciton and the polaron-pair are obtained. We will refer to these superpositions as *charge-transfer excitons*, hereafter CT excitons. The reader should note that the polaron-pair has been sometimes referred to as the charge-transfer exciton in the literature.²¹ The CT excitons, in their turn, have sometimes been called excimers.^{21,22,23} Our nomenclature is based on the most common usage of these terms, and we give precise quantum-mechanical definitions of these interchain species in section IV. One major difference between the work presented here and the existing literature is that we are also interested in *higher energy excited polaron-pairs and CT excitons*, which are defined exactly as above (thus, a high energy CT exciton is predominantly a superposition of a similar high energy excited intrachain exciton and polaron-pair). We find a 1:1 correspondence between the “essential states” that determine the photophysics of single strands^{29,30,31,32,33} and the dominant excited states including excited interchain species, that determine the photophysics of interacting chains.

Starting from a microscopic π -electron Hamiltonian, we investigate the energy spectrum of interacting PCP chains. We do not attempt to understand details of the photoluminescence (PL), which can be understood to a large extent within existing theories.^{17,21,22,23,25,26,27,28} Understanding delayed emission in PCP films (see below), on the other hand, will require much more sophisticated modeling. We rather focus on the theory of excited state absorption in interacting chains, with the goal of understanding the observed branching of photoexcitations and the origin of the polaronlike photoinduced absorptions (PAs),^{6,7,18,19} and experiments that indicate that in spite of the occurrence of these polaronlike PAs free charges are not generated as primary photoexcitations.^{34,35}

In the next section we present a brief yet detailed summary of relevant experiments in PCP films that indicate the strong role of interchain interactions, highlighting

in particular the apparently contradictory observations. Following this, in section III we present our theoretical model. In section IV we discuss the formation of CT excitons and excited state absorptions from them, and present detailed computational results. Finally, in section V we compare our theoretical results and experiments, and present our conclusions. The computational results presented in section III are for finite oligomers of PPV. In a separate Appendix we discuss the chain-length dependence of our results. We believe that our results apply to real materials.

II. REVIEW OF EXPERIMENTAL RESULTS

PL from films is often redshifted relative to that from dilute solutions, and the quantum efficiency (QE) of the PL from films is usually much smaller. PL from regioregular polythiophene (rrP3HT) has recently been discussed within a weak-coupling H-aggregate model, within which dipole-dipole coupling leads to an exciton band.¹⁷ Absorption here is to the highest state in the exciton band while emission is from the lowest state.^{17,25,27,28} Conversely, it has been claimed that PL from films of cyano-poly(paraphenylenevinylene), CN-PPV, and poly(2-methoxy,5-(2'-ethyl-hexyloxy)1,4-paraphenylenevinylene), MEH-PPV, are from CT excitons that occur below the intrachain optical exciton.^{9,10,21,22,23} Formation of CT excitons requires that polaron-pairs are energetically proximate to the excitons (see section IV and Appendix). The occurrence of low energy polaron-pairs is indicated by the observation of “persistent” or delayed PL lasting until milliseconds in films, the electric field quenching of the delayed PL, and the resumption of the PL upon removal of the field.^{1,2,11,12}

Experiments that also indicate the strong role of interchain interactions, and that are even more difficult to understand than PL involve transient absorption. Two distinct ultrafast photoinduced absorptions (PAs) are seen in solutions as well as in films with weak interchain interactions, such as dioctyloxy-poly-paraphenylenevinylene (DOO-PPV).^{36,37} The low energy PA₁ appears at a threshold energy of 0.7 eV and has a peak at ~ 1 eV, while the higher energy PA₂ occurs at ~ 1.3 – 1.4 eV. Comparison of PA and PL decays^{36,37} and other nonlinear spectroscopic measurements³⁸ have confirmed that these PAs are from the 1B_u optical exciton, in agreement with theoretical work on PCP single chains.^{29,30,31,32,33} In contrast, PA and PL in PCPs with significant interchain interactions (for e.g., MEH-PPV) are uncorrelated.^{1,6,7} It has been argued that PAs in such systems is from the polaron-pair.^{1,6,7} This would require generation of the polaron-pair in ultrafast time scales. The mechanism by which such ultrafast generation can occur is not clear.³⁹ The possibility that the PAs here are from the CT exciton has not been theoretically investigated.

Recent experiments have contributed further to the mystery. Sheng *et al.* have extended femtosecond (fs) PA measurements to previously inaccessible wavelengths,¹⁸ and have detected two additional weak PAs in film samples of MEH-PPV, PPV and rrP3HT that are absent in solutions of the PPV derivatives as well as in regiorandom (rraP3HT), which is known to have weaker interchain interaction than rrP3HT. The authors initially assigned the new low energy PA at ~ 0.35 – 0.4 eV, labeled P₁, and the higher energy PA, labeled P₂ in this work, to absorptions of free polarons that according to the authors are generated when interchain interactions are strong. The high energy PA associated with films had been previously observed in MEH-PPV,^{1,6,7} and it has been ascribed to absorptions from free polarons as well as from polaron-pairs.²⁰ Interestingly, these PAs peculiar to films are generated instantaneously, suggesting branching of photoexcitations with competing channels generating excitons and polarons. Such branching of photoexcitations would be in agreement with previous claim of the observation of infrared active vibrations (IRAV) in MEH-PPV in fs time,⁴⁰ but is difficult to reconcile with the large exciton binding energies deduced from PA₁ energy,^{29,36,38} which requires that polarons are generated from dissociation of the exciton due to extraneous influence at a later time. Instantaneous IRAV⁴⁰ has not been observed by other experimentalists, and interpretations other than those given by the original authors exist in the literature.⁴¹ In the context of Sheng *et al.*'s experiment, the following is, however, true: if the P₁ absorption, as well as the high energy absorption absent in solutions are indeed due to polarons, IRAV associated with these absorptions should have been observed. Intriguingly, Sheng *et al.* in their experiments did not find any IRAV at room temperatures that should have accompanied the P₁ absorption, and very weak IRAV at 80 K.¹⁸ Later more careful attempts have also failed to detect room temperature IRAV.⁴²

The absence of room temperature IRAV suggests that polarons are *not* being generated in Sheng *et al.*'s experiment. This conclusion is in apparent agreement with microwave conductivity measurements³⁴ and THz spectroscopy³⁵ that have found negligible polaron generation upon direct photoexcitation in both solutions and films. Based on very recent experiment that probed the polarization memory decay of photoexcitations, Singh *et al.* have concluded that the high energy PA associated with films is not from free polarons but from a CT exciton (note: these authors use the terminologies CT exciton and excimer synonymously).¹⁹ The origin of the polaronlike features in the PA thus remains mysterious.

III. THEORETICAL MODEL

Our calculations are within an extended two-chain Pariser-Parr-Pople Hamiltonian^{43,44} $H = H_{intra} + H_{inter}$, where H_{intra} and H_{inter} correspond to intra- and

interchain components, respectively. H_{intra} is written as,

$$H_{intra} = - \sum_{\mu, \langle ij \rangle, \sigma} t_{ij} (c_{\mu, i, \sigma}^\dagger c_{\mu, j, \sigma} + H.C.) + U \sum_{\mu, i} n_{\mu, i, \uparrow} n_{\mu, i, \downarrow} + \sum_{\mu, i < j} V_{ij} (n_{\mu, i} - 1)(n_{\mu, j} - 1) \quad (1)$$

where $c_{\nu, i, \sigma}^\dagger$ creates a π -electron of spin σ on carbon atom i of oligomer ν ($\nu = 1, 2$), $n_{\nu, i, \sigma} = c_{\nu, i, \sigma}^\dagger c_{\nu, i, \sigma}$ is the number of electrons on atom i of oligomer ν with spin σ and $n_{\nu, i} = \sum_{\sigma} n_{\nu, i, \sigma}$ is the total number of electrons on atom i . The hopping matrix element t_{ij} is restricted to nearest neighbors and in principle can contain electron-phonon interactions, although a rigid bond approximation is used here. U and V_{ij} are the on-site and intrachain intersite Coulomb interactions. We parametrize V_{ij} as⁴⁵

$$V_{ij} = \frac{U}{\kappa \sqrt{1 + 0.6117 R_{ij}^2}} \quad (2)$$

where R_{ij} is the distance between carbon atoms i and j in Å, and κ is the dielectric screening along the chain due to the medium. Based on previous work⁴⁵ we choose $U = 8$ eV and $\kappa = 2$. We write H_{inter} as

$$H_{inter} = H_{inter}^{1e} + H_{inter}^{ee} \quad (3)$$

$$H_{inter}^{1e} = -t_{\perp} \sum_{\nu < \nu', i, \sigma} (c_{\nu, i, \sigma}^\dagger c_{\nu', i, \sigma} + H.C.) \quad (4)$$

$$H_{inter}^{ee} = \frac{1}{2} \sum_{\nu < \nu', i, j} V_{ij}^{\perp} (n_{\nu, i} - 1)(n_{\nu', j} - 1) \quad (5)$$

We will assume planar cofacial stacking of oligomers in our calculations. While such ideal stacking does not occur in real systems, it is believed that this assumption captures the essential physics of polymer films.^{17,21,22,23,25,26,27,28} In the above, t_{\perp} is restricted to nearest interchain neighbors. We choose V_{ij}^{\perp} as in Eq. 2, with a background dielectric constant $\kappa_{\perp} \leq \kappa$.²²

IV. CHARGE-TRANSFER EXCITONS

A. Coupled ethylenes

In order to get a physical understanding of the effect of H_{inter} , we begin with the case of two ethylene molecules, placed cofacially one on top of the other such that the overall structure has a center of inversion. The small number of energy states here permit clear identification of all two-chain excitations. Although full configuration interaction (FCI) can be performed in this case, in view of our interest in long PPV oligomers, we will restrict our calculations as well as physical discussions to the single configuration interaction (SCI) approximation (see, however, section IV.D.)

We consider first the $U = V_{ij} = 0$ molecular orbital (MO) limit for H_{intra} . The ethylene MOs are written as,

$$a_{\nu, \lambda, \sigma}^\dagger = \frac{1}{\sqrt{2}} [c_{\nu, 1, \sigma}^\dagger + (-1)^{(\lambda-1)} c_{\nu, 2, \sigma}^\dagger] \quad (6)$$

where $\lambda = 1(2)$ corresponds to the bonding (antibonding) MO. The spin singlet one-excitation space for the two molecules consists of four configurations. Two of these four configurations consist of neutral molecules, with either of the two molecules excited and the other in the ground state; the other two consist of positively and negatively charged molecules, with each charged molecule in its lowest state. We refer to the neutral configurations with intramolecular excitations as excitons, and write them as $|exc1\rangle$ and $|exc2\rangle$, ignoring for the moment that true excitons require nonzero U and V_{ij} . We will refer to the charged molecule pair as polaron-pairs and write them as $|P_1^+ P_2^-\rangle$ and $|P_1^- P_2^+\rangle$, respectively. The exciton and polaron-pair wavefunctions are given by,

$$|exc1\rangle = \frac{1}{\sqrt{2}} a_{2, 1, \uparrow}^\dagger a_{2, 1, \downarrow}^\dagger (a_{1, 1, \uparrow}^\dagger a_{1, 2, \downarrow}^\dagger - a_{1, 1, \downarrow}^\dagger a_{1, 2, \uparrow}^\dagger) |0\rangle \quad (7)$$

$$|P_1^+ P_2^-\rangle = \frac{1}{\sqrt{2}} a_{2, 1, \uparrow}^\dagger a_{2, 1, \downarrow}^\dagger (a_{1, 1, \uparrow}^\dagger a_{2, 2, \downarrow}^\dagger - a_{1, 1, \downarrow}^\dagger a_{2, 2, \uparrow}^\dagger) |0\rangle \quad (8)$$

The terms within the parenthesis in Eqs (7) and (8) constitute singlet bonds between MOs. The basis functions $|exc2\rangle$ and $|P_1^- P_2^+\rangle$ are obtained from the above by applying mirror-plane symmetry. The four spin-bonded valence bond (VB) diagrams corresponding to the excitons and polaron-pairs are shown in Fig. 1(a).

Nonzero H_{inter} mixes these pure states to give the CT excitons,^{21,22,23} the theory of which is fundamentally similar to the Mulliken's theory of ground state charge-transfer⁴⁷ (except that the excited state Hamiltonian for identical molecules involves four instead of two basis functions). Consider first the $H_{inter}^{1e} = 0$ limit. Matrix elements of H_{inter}^{ee} are zero between $|P_1^+ P_2^-\rangle$ and $|P_1^- P_2^+\rangle$ but nonzero between $|exc1\rangle$ and $|exc2\rangle$, indicating that while the polaron-pair states are degenerate for $H_{inter}^{ee} \neq 0$, the exciton states form new nondegenerate states $|exc1\rangle \pm |exc2\rangle$ (see Fig. 1(b)). The dipole operator $\boldsymbol{\mu} = e \sum_{\nu, i} \mathbf{r}_{\nu, i} (n_{\nu, i} - 1)$, where $\mathbf{r}_{\nu, i}$ gives the location of atom i on oligomer ν , couples the ground state to only the even parity exciton state. The odd parity exciton is now a dark state occurring below the optical exciton. The splitting of the exciton states due to Coulomb interactions alone can be described within the dipole-dipole approximation.^{17,25,26,27,28}

We now switch on H_{inter}^{1e} , which mixes the odd parity neutral $|exc1\rangle - |exc2\rangle$ and charged $|P_1^+ P_2^-\rangle - |P_1^- P_2^+\rangle$, to give the two CT exciton states in Fig. 1(c). The extent of configuration mixing depends on the relative energy separation between the pure polaron-pair and the odd parity exciton in Fig. 1(b) and the magnitude of H_{inter}^{1e} , i.e., on V_{ij}^{\perp}/t_{\perp} . For significant V_{ij}^{\perp} (attraction between

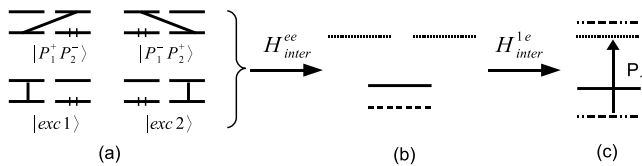


FIG. 1: (a). The one-excitation space of two weakly interacting oligomers. For each oligomer one bonding and one antibonding MO is shown. The MOs can be occupied by 0, 1 or 2 electrons. The singly occupied MOs are connected by singlet bonds. (b) and (c). Eigenstates of H_{inter}^{ee} and total H_{inter} , respectively. Solid lines, even parity exciton; dashed line, odd parity exciton; dot-dashed lines, CT excitons; dotted lines, polaron-pairs. The P_1 induced absorption is indicated in (c).

interchain electron and hole), the polaron-pair can be low in energy (see Appendix). The CT excitons, being superpositions of the dark exciton state and odd parity polaron-pair configurations, neither of which are accessible in intramolecular optical excitation, are optically forbidden from the ground state. The even parity states, the optical exciton $|exc1\rangle + |exc2\rangle$ and the polaron-pair $|P_1^+ P_2^- \rangle + |P_1^- P_2^+ \rangle$, are not affected by H_{inter}^{1e} in this symmetric case.

We now make an observation that will be central to the work presented in the next sections: matrix elements of the *transverse* component of $\boldsymbol{\mu}$, perpendicular to the molecular axes, between the CT excitons and the even-parity polaron state are nonzero, and proportional to t_{\perp} . For nonzero t_{\perp} we therefore expect *excited state charge-transfer absorption* from the CT exciton to the polaron-pair state, the strength of which is proportional to $t_{\perp}^2/\Delta E$, where ΔE is the energy difference between the initial and final states.⁴⁷ This is shown explicitly in the next section. We label this photoinduced CT absorption as P_1 , as we will show that it is this induced absorption in the context of PCPs that corresponds to the PA labeled P_1 by Sheng *et al.*¹⁸

The above discussion starts from the $U = V_{ij} = 0$ limit of H_{intra} only for simplicity. For the particular case of two ethylenes, the two neutral exciton configurations are the same, independent of U and V_{ij} . The description of the polaron-pair states also remains the same within the SCI approximation (higher energy two electron-two hole excitations can modify the polaron-pair states in approximations that go beyond SCI). For nonzero U and V_{ij} , the dominant contribution to the stabilization of the lower CT exciton still comes from the configuration mixing with the odd-parity polaron-pair basis function. The strength of the dipole-coupling between the CT exciton and the even-parity pure polaron-pair state, the P_1 absorption in Fig. 1(c), is again $t_{\perp}^2/\Delta E$, where, however, ΔE now depends on U and V_{ij} .

B. Cofacial PPV oligomers, symmetric case

We now go beyond the two ethylenes and make the following observations.

(i) Eqs. 7 and 8, or equivalently, the four spin-bonded VB diagrams in Fig. 1(a), with the MOs corresponding to the highest occupied and lowest unoccupied MOs (HOMOs and LUMOs), describe the lowest intramolecular excitations and the lowest energy polaron-pair states for arbitrary PCP oligomers in the $U = V_{ij} = 0$ limit of H_{intra} . For extension of the above concept to arbitrary PCPs, only Eq. 6 needs to be modified, with the MOs now superpositions of a larger number of atomic wavefunctions. The degenerate neutral exciton states are once again split by the Coulomb interactions in H_{inter} alone, even for $t_{\perp} = 0$, as in Fig. 1(b). This is the basis for the dipole-dipole approximation to exciton splitting.^{17,25,26,27,28}

The dipole-dipole approximation, or more precisely, the $t_{\perp} = 0$ approximation, ignores the CT between the odd parity polaron-pair and exciton states. The extent of this CT, as pointed out in the above, depends on the magnitude of the *effective* electron hopping between the MOs of the two interacting oligomers, and the energy separation between the pure odd parity polaron-pair and exciton states in the $t_{\perp} = 0$ limit. The energy separation between the polaron-pair and the exciton depends on the difference in the electron-hole separations in the intrachain exciton and the polaron-pair, a quantity difficult to evaluate from first principles. The relative energy difference between the polaron-pair and the exciton in theoretical work can therefore be based only on interpretations of experiments. The likelihood of short electron-hole separations in the polaron-pair (and therefore energy close to the exciton, which in turn increases CT) has been suggested by several authors. Based on the work reported in references 1 and 2, Wu and Conwell,^{21,22} and Meng²³ have previously assumed low energy polaron-pair states, and have described the CT process in PPV derivatives within a simplified H_{inter}^{ee} , in order to explain the reduced PL in films (indeed, references 11 and 12 suggest that a fraction of the polaron-pair states occur even *below* the exciton). We have found in our calculations that for $k_{\perp} \leq 2.5$ (see Eqs. 2 and 5) the fundamental assumption of Wu and Conwell and Meng continues to be valid for long chains of polyenes and PPVs (see Appendix), and we adopt the same approach.

To conclude, Fig. 1 applies to the $U = V_{ij} = 0$ limit of arbitrary PCPs, when the excitations involve the HOMO and LUMO of the two identical cofacial oligomers. We have verified this from CI calculations with $H_{intra} = 0$ but $H_{inter} \neq 0$ for long PPV oligomers. The energy splitting between the exciton and the CT exciton is relatively insensitive to chain length. To identify wavefunctions as polaron-pair, CT exciton, etc., we choose an orbital set consisting of the Hartree-Fock orbitals of the individual molecular units, and perform CI calculations using these localized MOs. The localized basis allows calculations

TABLE I: SCI excited states of two symmetrically placed 8-unit PPV oligomers for $\kappa_{\perp} = 2$, $t_{\perp} = 0.1$ eV. Here j and E_j are quantum numbers (without considering symmetry) and energy, respectively. Ionicity is the charge on the chains. The states are arranged not according to their energies, but according to the manifolds they belong to (see text). The $\mu_{G,j}$ and $\mu_{i,j}$ are the dipole couplings (electronic charge = 1) between the ground state and state j , and between excited states, respectively.

j	E_j (eV)	Ionicity	$\mu_{G,j}$	$\mu_{i,j}$
2	2.67	0.26	0	—
4	2.81	0	6.52	—
5	3.00	1	0	2.04 ^a
8	3.12	0.74	0	—
3	2.81	0.29	0	—
7	3.06	0	0	—
9	3.12	1	0	—
10	3.24	0.64	0	—
11	3.26	0.38	0	6.91 ^b
15	3.42	0	0	6.83 ^{b,c}
19	3.46	1	0	7.68 ^b
26	3.67	0.55	0	6.69 ^b

^a $i=2$. ^bAll dipole couplings are with states in lowest manifold near $1B_u$ with the same character (see text). ^c The mA_g .

of ionicities of individual oligomers. The expected ionicities are 0 and 1 for the exciton and the polaron-pair, respectively, and fractional for the CT excitons.

(ii) There is no *a priori* reason to assume that the MOs in Fig. 1 should include only the HOMOs and the LUMOs of the PCP oligomers. *Higher energy excited exciton and polaron-pair states*, involving bonding (anti-bonding) MOs below (above) the HOMO (LUMO), can also be coupled by H_{inter} , provided once again, the excited polaron-pairs and the excitons are close in energy. Again, we have confirmed this from CI calculations in the $H_{intra} = 0$, $H_{inter} \neq 0$ limit for PPV oligomers, using the localized basis.

(iii) The results of (i) and (ii) indicate that for $U = V_{ij} = 0$ but $H_{inter} \neq 0$, the two-chain energy spectrum consists of a series of overlapping energy manifolds, with each manifold containing an exciton, a polaron-pair and two CT excitons, as in Fig. 1(c). For nonzero U and V_{ij} , single chain excited eigenstates are superpositions of the single chain MO configurations. It is therefore reasonable to speculate that the two-chain spectrum for *nonzero* U and V_{ij} also consists of similar energy manifolds, at least upto the continuum band. We have verified this, using the localized MO basis set and the SCI approximation, including *all* one-excitations, within the complete two-chain Hamiltonian. We have summarized our results for two interacting symmetrically placed cofacial 8-unit PPV oligomers at a distance of 0.4 nm in Table I, where we

TABLE II: SCI eigenstates of cofacial PPV oligomers of lengths 7 and 9-units, respectively, with only one end matching. All parameters are the same as in Table I. The classifications of states in the last column are obtained from wavefunction analysis (see text)

j	E_j (eV)	Ionicity	$\mu_{G,j}$	$\mu_{i,j}$	state type
2	2.67	0.25	0.78	—	CT exciton
3	2.81	0.11	4.99	—	exciton
4	2.87	0.16	4.17	—	exciton
6	3.01	1.00	0.00	2.03 ^a	polaron-pair
7	3.13	0.31	0.19	—	CT exciton
5	2.99	0.13	0.04	—	two-photon exciton
8	3.13	0.68	0.09	—	CT exciton
9	3.15	0.99	0.00	—	polaron-pair
10	3.20	0.15	1.42	—	CT exciton
11	3.28	0.38	0.00	6.75 ^b	mA_g CT exciton
15	3.41	0.16	0.00	6.30 ^b	mA_g exciton
17	3.47	0.19	0.00	5.96 ^b	mA_g exciton
18	3.50	0.69	0.24	4.77 ^b	mA_g “polaron-pair”
19	3.52	0.62	0.76	3.42 ^b	mA_g “polaron-pair”

^a $i=2$. ^bAll dipole couplings are with states in lowest manifold near $1B_u$ with the same character.

have clearly indicated the different energy manifolds. Intrachain one- or two-photon excitons, interchain polaron-pairs and CT excitons within each manifold are easily identified from their ionicities and transition dipole couplings, even at higher energies.

C. Cofacial PPV oligomers: unsymmetric case

We now relax the inversion symmetry condition to take disorder into account approximately. This is important, as with nonzero interchain hopping, it is not obvious that the characterizations of eigenstates as intrachain excitons, CT excitons and polaron-pairs continue to be true at higher energies in the absence of perfect symmetry. Furthermore, we will see that such disorder also accounts for the appearance of instantaneous signature of the PA P_1 .¹⁸ We consider cofacial oligomers of different lengths, with only one end matching (see insert, Fig. 2). In Table II we show the results of SCI calculations for PPV oligomers 7- and 9-units long, 0.4 nm apart. We have verified that these results are independent of the actual lengths of the oligomers, by performing similar calculations for pairs of oligomers of different lengths ranging from 5 to 10 units. Unlike Table I, here we have given also the dominant character, intrachain exciton, CT exciton or polaron-pair of each eigenstate.

As indicated in Table II, in the absence of inversion symmetry, characterizations of eigenstates requires going

beyond ionicities. We determine the dominant characters the eigenstates from detailed wavefunction analysis. For example, the $j = 2$ state in Table II has large overlaps with the odd parity configurations $|exc1\rangle - |exc2\rangle$ and $|P_1^+P_2^-\rangle - |P_2^+P_1^-\rangle$, and very weak overlap with the even parity $|exc1\rangle + |exc2\rangle$, identifying this state as predominantly a CT exciton. Exactly the opposite is true for states $j = 3$ and 4, which are the intrachain excitons. The states $j = 3$ and 4 also have weak but nonzero overlaps with the even parity $|P_1^+P_2^-\rangle + |P_2^+P_1^-\rangle$, which gives them weak ionic character. The occurrence of two distinct optical exciton states, split by a very small energy difference, is a consequence of asymmetry. This characterization is in agreement with their large dipole couplings to the ground state, as well as small ionicities. Another consequence of asymmetry is that the CT exciton is now weakly dipole-coupled to the ground state (the relative contributions to the wavefunction of $|exc1\rangle$ and $|exc2\rangle$ are unequal), indicating weak but direct photogeneration of this state from the ground state. The polaron-pair state in the lowest manifold ($j = 6$) can be still identified by its ionicity alone. Wavefunction analysis here indicates this state to be an even superposition of $|P_1^+P_2^-\rangle$ and $|P_1^-P_2^+\rangle$. Exactly as in Table I we find nonzero transition dipole-coupling between the $j = 1$ CT exciton and the polaron-pair, with the magnitude of the coupling nearly the same. Furthermore, the CT exciton continues to have zero transition dipole coupling with all other states in this manifold.

The characterizations of the states in the second and third energy manifolds are obtained similarly from calculations of overlaps with the fundamental basis functions. These basis functions, however, involve higher energy single-particle excitations orthogonal to those contributing to the states in the lower manifold (for example, the excitonic basis functions contributing to the $j = 5$ state in Table II has strong contributions from the HOMO \rightarrow LUMO+2 and HOMO $- 1 \rightarrow$ LUMO contributions of each chain, identifying it as a two-photon exciton.) The energy orderings within the manifolds can also be different from that in the lowest manifold. Thus the ordering of the lowest intrachain and CT excitons are reversed in the second manifold, with the lower energy $j = 5$ being the intrachain exciton and the higher energy $j = 8$ being the CT exciton. We comment on the states labeled mA_g in the third manifold in Table II in the next subsection. Here we only point out that the $j = 18$ and 19 states, in spite of their intermediate ionicities, are predominantly polaron-pair, based on their strong overlaps with even superpositions of high energy charged configurations. The strong mixing between intrachain and interchain basis functions in this region is a signature that this energy region is close to the continuum band.²⁹

To summarize this subsection, characterizations of eigenstates as predominantly intrachain exciton, CT exciton and polaron-pair continues to be valid even in the presence of disorder, although they become less appropriate at higher energies.

D. Photoinduced absorptions

Besides energies and ionicities, Tables I and II also list the transition dipole couplings of excited states with the ground state, and between the excited states themselves. The key results of Tables I and II are: (i) direct photogenerations of the optical exciton and the two lowest CT excitons, one below and one above the intrachain exciton, are allowed in the presence of disorder, and (ii) the lowest CT exciton plays a crucial role in PCP films. We have verified that our results remain qualitatively intact for three or more oligomers, different relative orientations and distances.

The intrachain exciton states in the third manifolds, $j = 15$ in Table I and $j = 15$ and 17 in Table II correspond to the single chain mA_g exciton, which is the two-photon state that dominates single-chain photophysics.^{29,30,31,32} PA_1 in solutions is to the mA_g .³³ Our calculations indicate that exactly as the transition dipole coupling is large between the single-chain $1B_u$ and the single-chain mA_g ,²⁹ equally large dipole couplings occur between pairs of states in the $1B_u$ and mA_g manifolds that are of the same character (for example, from the CT exciton in the $1B_u$ manifold to the CT exciton in the mA_g manifold).

In Fig. 2 we compare PAs calculated for a single 8-unit PPV oligomer with that from the lowest CT exciton in a two-chain system consisting of a 7-unit and a 9-unit oligomer. We have shown results for three different parameter sets to indicate the relative insensitivity of our results to parameters. We performed similar calculations for many other combinations of chain lengths involving PPV oligomers of lengths from 5 to 10 units. There is very little difference between the different cases (except that in the symmetric cases the CT exciton has zero transition dipole coupling with the ground state). PA_1 in the single chain corresponds to the transition from the $1B_u$ to the mA_g . The initial and final states of PA'_1 absorptions in the two-chain systems are both CT excitons. The P_1 absorption, missing in the single chain, is from the lowest CT exciton to the lowest polaron-pair. The calculated PAs for the two-chain system are *excited state equivalents* of the absorptions expected within the classic Mulliken theory of weak donor-acceptor complexes. In a donor-acceptor complex, there occurs weak CT absorption at low energy, in addition to the molecular absorptions.⁴⁷ In Fig. 2, P_1 is the CT absorption and PA'_1 the molecular absorption.

Sheng *et al.*,¹⁸ and more recently, Singh *et al.*¹⁹ have also discussed a higher energy PA, above PA'_1 , peculiar to films. It is believed¹⁹ that this high energy PA is the same that was observed very early in MEH-PPV.^{6,7} As discussed before in the context of the PA_2 absorption in single chains,³³ such high energy regions cannot be investigated within the SCI approximation, and higher order CI calculations become essential. Such calculations for pairs of PPV oligomers is beyond our capability currently. On the other hand, as emphasized in section

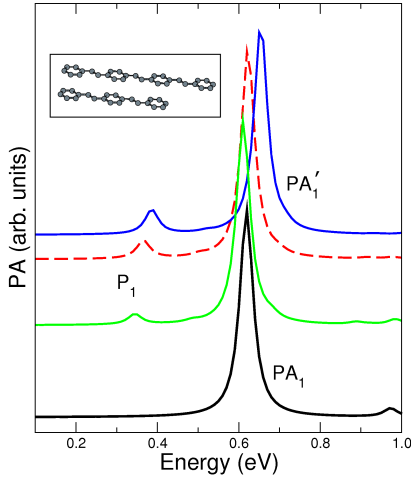


FIG. 2: (Color online) Calculated PAs for a 8-unit PPV oligomer (black curve), and for a two-chain system consisting of a 7-unit and a 9-unit oligomer: for $\kappa_{\perp} = 2$ and $t_{\perp} = 0.1$ eV (green); $\kappa_{\perp} = 1.75$ and $t_{\perp} = 0.15$ eV (red); and $\kappa_{\perp} = 1.5$ and $t_{\perp} = 0.2$ eV (blue). A linewidth of 0.02 eV is assumed in all cases. The inset shows schematically the arrangement of the oligomers, with the ends matching on one side only. PA_1 is from the exciton. P_1 and PA_1' are from the CT exciton.

IV.A, the photophysics of the CT exciton in PCPs can be anticipated even from the behavior of coupled ethylene molecules. We have performed FCI calculations for pairs of ethylene and butadiene molecules and have indeed detected a high energy two-electron two-hole polaron-pair state $|P_1^+ P_2^- - P_2^+ P_1^- \rangle_{2e-2h}$ to which absorption from the CT exciton is allowed. In the notation of section III, the components of this state for the coupled ethylene system are,

$$|P_1^+ P_2^- \rangle_{2e-2h} = \frac{1}{2} [a_{2,2,\uparrow}^\dagger a_{2,2,\downarrow}^\dagger (a_{1,1,\uparrow}^\dagger a_{2,1,\downarrow}^\dagger - a_{1,1,\downarrow}^\dagger a_{2,1,\uparrow}^\dagger) + a_{2,1,\uparrow}^\dagger a_{2,1,\downarrow}^\dagger (a_{1,2,\uparrow}^\dagger a_{2,2,\downarrow}^\dagger - a_{1,2,\downarrow}^\dagger a_{2,2,\uparrow}^\dagger)] |0\rangle \quad (9)$$

$$|P_2^+ P_1^- \rangle_{2e-2h} = \frac{1}{2} [a_{1,2,\uparrow}^\dagger a_{1,2,\downarrow}^\dagger (a_{1,1,\uparrow}^\dagger a_{2,1,\downarrow}^\dagger - a_{1,1,\downarrow}^\dagger a_{2,1,\uparrow}^\dagger) + a_{1,1,\uparrow}^\dagger a_{1,1,\downarrow}^\dagger (a_{1,2,\uparrow}^\dagger a_{2,2,\downarrow}^\dagger - a_{1,2,\downarrow}^\dagger a_{2,2,\uparrow}^\dagger)] |0\rangle \quad (10)$$

Each polaron-pair configuration now has two components, related by electron-hole symmetry. In Figs. 3(a) and (b) we have shown the four spin bonded VB diagrams that describe this high energy polaron-pair state. The diagrams are similar for coupled butadienes, with the only difference that there occur now bonding (antibonding) MOs below (above) the bonding (antibonding) MOs of Fig.3.

It is easy to see why charge-transfer absorption to this state from the CT exciton is allowed for nonzero t_{\perp} . Within the exciton representation such an absorption originates from interunit charge-transfer from either frontier MO of one unit to either frontier MO of the second

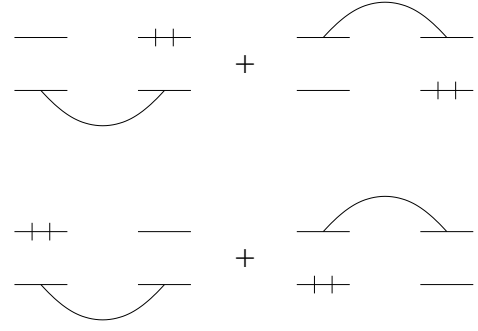


FIG. 3: Two electron - two hole excitations of two weakly interacting ethylene molecules that are reached by optical absorption from the CT exciton of Fig. 1(c). The spin singlet diagrams shown are excited polaron-pair states corresponding to Eqs. (9) and (10), respectively, with each molecule having unit positive or negative charge.

unit.⁴⁶ One can then have low energy charge-transfer, from the occupied antibonding MOs of the intrachain excitons in Fig. 1(a) to the unoccupied antibonding MOs of the neighboring unit, creating the low energy polaron-pair state discussed in section IV.A. This is the P_1 absorption. In addition, it is possible to have transition from the the singly occupied (doubly occupied) bonding MO of one unit of the forbidden exciton to the unoccupied (singly occupied) antibonding MO of the neighboring unit. This second transition is clearly at higher energy, and gives the excited polaron-pair states of Figs. 3(a) and (b). In spite of the basic similarity between ground state and excited state charge-transfer, there then does exist one fundamental difference between them, viz., multiple charge-transfer absorptions will occur in the latter case, as opposed to a single absorption in the former.

E. Finite oligomers versus polymers

One possible criticism of the work presented above might be that the calculations are for finite oligomers and therefore they may not apply to infinite chains. Different research groups have shown, for instance, that within the dipole-dipole interaction model the splitting between the optical and the dark exciton vanishes in the infinite chain length.^{17,25,28} We point out the following in this context. First, the dipole-dipole interaction model is valid only when the polaron-pair configuration is ignored ($t_{\perp} \rightarrow 0$ limit). For reasonable t_{\perp} and V_{ij}^{\dagger} , the stabilization of the dark exciton comes predominantly from CI with the polaron-pair (see Appendix). Second, real PCPs are not true infinite chains and usually consist of a distribution of conjugation lengths that are close to what we have considered here.^{39,45} As seen in the Appendix, the energy gap between the optical and the CT exciton does indeed decrease with size, but there is a broad region over which this gap is nearly the same. Third, and most important in the present context, it is not the gap between the optical

exciton and the CT exciton, but rather, *the gap between the polaron-pair and the CT exciton*, that is relevant for our theory. We show in the Appendix that this second gap, corresponding to the P_1 transition energy, increases weakly with increasing size.

V. DISCUSSIONS AND COMPARISON TO EXPERIMENTS

Our work provides the insight necessary to understand the various mutually contradictory experimental results. There occur in PCPs a series of interchain CT excitons and polaron-pairs in the energy space below the continuum band. The lowest CT exciton occurs below the optical exciton, and its wavefunction is a superposition of (a) the wavefunction of the lowest state in the exciton band of a H-aggregate, and (b) the lowest polaron-pair state of odd parity. The disorder-induced 0-0 emission, as well as the 0-1 emission from the lowest H-aggregate state and from the CT exciton are therefore very likely similar, since the polaron-pair component of the CT exciton has no dipole coupling with the ground state and should not interfere in the emission process. The success of the H-aggregate model in explaining the PL of rrP3HT^{17,27} therefore does not contradict the CT exciton scenario. As emphasized by others,⁸ probing at a variety of wavelengths is essential for understanding the complete role of morphology.

Whether or not significant CT occurs in real systems depends on the magnitude of t_{\perp} and the relative energies of the dark exciton and the polaron-pair in the absence of t_{\perp} . The demonstration of delocalized two-dimensional polarons in rrP3HT⁴⁸ proves that t_{\perp} should be large enough for interchain electron hopping. Similar large t_{\perp} has been assumed in calculations for CN-PPV and MEH-PPV^{21,22,23}. As mentioned already, delayed PL in films is cited as evidence for some polaron-pairs occurring even below the optical exciton^{1,2} (it is not being implied that these polaron-pairs are generated in photoexcitation.) This would suggest that even though the bulk of the polaron-pairs are above the exciton, they are proximate in energy (see also Appendix). Taken together, moderate t_{\perp} and relatively low energy polaron-pairs indicates significant charge-transfer.

Within our theory, PA in films is from both the CT exciton and the optical exciton at the earliest times, and predominantly from the CT exciton following this. The similarity between the two-chain PA in Fig. 2 and the low energy part of the experimental PA spectra of by Sheng *et al.*¹⁸ is striking. PA_1 in solutions is the absorption from the single-chain $1B_u$ to the mA_g . As in Sheng *et al.*'s experiment for solutions, the P_1 absorption is missing in our single chain calculation. The P_1 absorption in films, however, is not from free polarons, but is a charge-transfer absorption from the lowest CT exciton to the lowest polaron-pair. PA in the 1 eV range in solutions and films appear to be identical but have slightly differ-

ent origins: in films this is the PA'_1 absorption from the lowest CT exciton to a higher energy CT exciton in the mA_g - manifold. The branching of photoexcitations, as discussed by Sheng *et al.*, is real, and the instantaneous generation of P_1 is likely a consequence of the CT exciton being weakly allowed in absorption due to disorder. Our theory is a straightforward extension of Mulliken's theory of ground state charge-transfer in a donor-acceptor complex⁴⁷ to the case of photoinduced charge-transfer in PCP films. As in Mulliken's theory, there occur from the CT exciton charge-transfer absorptions (*viz.*, P_1 in Fig. 2) absent in the pure "molecular" components, in addition to the weakly perturbed "molecular absorption" PA'_1 .

Our interpretation of P_1 explains the absence of room temperature IRAV in Sheng *et al.*'s photoexcitation experiment, since free charges are not generated. The weak low temperature IRAV may owe its origin to the polaron-pair contributions to the CT exciton wavefunction. In the disordered case, the contributions by $|exc1\rangle$ and $|exc2\rangle$, and by $|P_1^+P_2^-\rangle$ and $|P_1^-P_2^+\rangle$, respectively, to the CT exciton are different, and this asymmetry may make weak IRAV possible. This is currently being investigated. The apparent contradiction between ultrafast spectroscopy on the one hand, and microwave³⁴ and THz spectroscopy³⁵ on the other, is also understandable once it is recognized that P_1 is not associated with polarons.

The PA_2 seen in solutions is a second higher energy "molecular absorption", and from the above extension of Mulliken theory, we expect a weakly perturbed PA'_2 absorption in films. We have not tried to directly evaluate this PA, as even in single chains the understanding of PA_2 requires highly sophisticated many-body calculations.³³ Similar calculations are currently beyond our reach for the two-chain case, but the results of Tables I and II indicate that the interchain species that is the final state of PA'_2 must exist. More interesting is the higher energy PA peculiar to films and absent in solutions.^{6,7,18,19} We have not calculated this higher energy PA for PPV oligomers, but have determined that such an absorption from the CT exciton is found in FCI calculations on coupled ethylene and butadiene chains. The analogy between coupled ethylenes and long PCP chains pointed out in section IV suggest that similar high energy two electron - two hole polaron-pair state will exist also in arbitrary PCPs. Based on the very slow polarization memory decay kinetics, the high energy PA associated with films has recently been ascribed to absorption from the CT exciton,¹⁹ in agreement with our prediction.

Our calculations allow us to make predictions for polarizations of the PAs. We predict that PA'_1 in films will be polarized along the PCP chains, and that P_1 will be polarized transverse to the chains. Preliminary polarization memory measurements are in agreement with these predictions, but more careful measurements have to be performed to confirm that the PAs are from the same species.⁴² Finally, CT excitons have also been claimed in recent experiments on dendritic oligothiophenes⁴⁹ and in

pentacene films.⁵⁰

While the present theoretical work has focused entirely on single-component PCPs, several experimental groups have recently discussed charge-transfer complexes (CTCs) created upon photoexcitations of heterstructures composed of donors and acceptors.^{51,52,53,54} The donor-acceptor polaron-pair as well as the CTC here are expected and found below the optical gaps of the donor as well as the acceptor. Theoretical work on excited state absorptions from the CTCs⁵⁴ is of interest and is currently being pursued.

Acknowledgments

S. M. thanks Z. V. Vardeny for suggesting this work and for the hospitality extended by the University of Utah where this work was conceived. We are grateful to L. J. Rothberg and C.-X. Sheng for many stimulating discussions and for sending preprints. This work was supported by NSF-DMR-0705163.

APPENDIX

In order to understand finite size effects associated with our results we have calculated the energy spectra near the optical gap edge for pairs of linear polyenes as well as for PPV oligomers for many different chain lengths. In Fig. 4(a) we show our results for pairs of cofacial linear polyenes for $\kappa_{\perp} = 2.5$. The number of carbon atoms per chain N ranges from 10 to 70. The energy orderings are the same as in Fig. 1. We show plots of (i) the energy difference between the optical exciton and the dark exciton, ΔE_{e-e} and (ii) the energy difference between the polaron-pair and the CT exciton, ΔE_{pp-e} . We have chosen larger κ_{\perp} than in Tables I and II (weaker interchain electron-hole attraction) since for $\kappa < 2$ the polaron-pair and the CT exciton are both too low in energy at small N , and the ionicity of the CT exciton is much larger than in Tables I and II. For $\kappa_{\perp} = 2.5$ the ionicities are comparable. Our results for ΔE_{e-e} should be compared against those obtained using the supermolecular approach in reference 26 (see Fig. 2(a) of this reference which shows results for interchain separation of 0.45 nm). For the same N values, the ΔE_{e-e} are comparable. We have plotted our energy differences against N rather than $1/N$ to point out that although

ΔE_{e-e} indeed decreases with N , there is a broad range of N where the decrease is slow. For real polyacetylene films we expect $\Delta E_{e-e} \neq 0$.

The plots for ΔE_{e-e} and ΔE_{pp-e} are not completely independent. As seen in the figure, decreasing ΔE_{e-e} is accompanied by increasing ΔE_{pp-e} , which is a signature that the bulk of the stabilization of the CT exciton is coming from CI with the polaron-pair (the CI decreases with increasing energy of the of the polaron-pair). Again, ΔE_{pp-e} is nearly the same over a broad range of N .

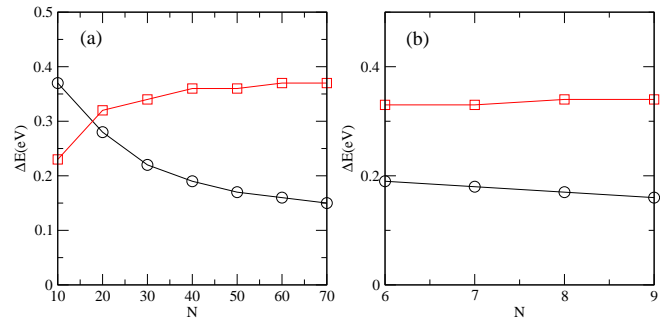


FIG. 4: Energy difference between the optical and CT exciton (circles), and between the polaron-pair and the CT exciton (squares) in pairs of (a) linear polyenes, (b) PPV oligomers.

In Fig. 4(b) we have shown the same results for PPV oligomers with $\kappa_{\perp} = 2$, with N now the number of units as opposed to number of carbon atoms. Again, our results for ΔE_{e-e} should be compared against Fig. 3 of reference 25, where, however, the calculations go up to 7 units only. As in Fig. 4(a), the plots against N (as opposed against $1/N$) make the slow variation of the energy differences against size clear. Decreasing ΔE_{e-e} is accompanied by increasing ΔE_{pp-e} , as in Fig. 4(a).

Finally, it is not being implied that the actual magnitudes of the calculated energy differences should be taken seriously. The quantitative aspects of the calculations depend to a large extent on the parametrization of V_{ij} and V_{ij}^{\perp} , which are not known. Equally importantly, the effects of background polarization are difficult to estimate. It may, however, be significant that our parametrization⁴⁵ of V_{ij} has given the most accurate estimations of exciton energies and exciton binding energies in a different family of π -conjugated systems, viz., single-walled carbon nanotubes, to date.⁵⁵

¹ L. Rothberg, in *Semiconducting Polymers: Chemistry, Physics and Engineering, Vol. I*, Edited by G. Hadziioannou and G.G. Malliaras (John Wiley, 2006), and references therein.

² V. I. Arkhipov and H. Bässler, *Phys. Stat. Sol.(a)* **201**, 1152 (2004), and references therein.

³ B. J. Schwartz, *Annu. Rev. Phys. Chem.* **54**, 141 (2003),

and references therein.

⁴ S. A. Jenekhe and J. A. Osaheni, *Science* **265**, 765 (1994).

⁵ S. A. Jenekhe, *Adv. Mater.* **7**, 309 (1995).

⁶ M. Yan, L. J. Rothberg, F. Papadimitrakopoulos, M. E. Galvin and T.M. Miller, *Phys. Rev. Lett.* **72**, 1104–1107 (1994).

⁷ J. W. P. Hsu, M. Yan, T.M. Jedju, L.J. Rothberg and B.R.

- Hsieh, Phys. Rev. B **49**, 712–715 (1994).
- ⁸ I. B. Martini, A. D. Smith and B. J. Schwartz, Phys. Rev. B **69**, 035204 (2004).
 - ⁹ I. D. W. Samuel, G. Rumbles and C. J. Collison, Phys. Rev. B **52**, R11573 - R11576 (1995).
 - ¹⁰ I. D. W. Samuel, G. Rumbles, C. J. Collison, S. C. Moratti and A. B. Holmes, Chem. Phys. **227**, 75 (1998).
 - ¹¹ B. Schweitzer, V. I. Arkhipov and H. Bässler, “ Chem. Phys. Lett. **304**, 365 (1999).
 - ¹² D. Hertel, Y. V. Romanovskii, B. Schweitzer, U. Scherf and H. Bässler, Synth. Metals **116**, 139 (2001).
 - ¹³ P. K. H. Ho, J. -S. Kim, N. Tessler and R. H. Friend, J. Chem. Phys. **115**, 2709 (2001).
 - ¹⁴ S.-H. Lim, T. G. Björklund, K. M. Gaab and C. J. Bardeen, J. Chem. Phys. **117**, 454 (2002).
 - ¹⁵ P. J. Brown, D. S. Thomas, A. Köhler, J. S. Wilson, J. -S. Kim, C. M. Ramsdale, H. Siringhaus and R. H. Friend, Phys. Rev. B **67**, 064203 (2003).
 - ¹⁶ A. B. Koren, M. D. Curtis, A. H. Francis and J. W. Kampf, J. Am. Chem. Soc. **125**, 5040 (2003).
 - ¹⁷ J. Clark, C. Silva, R. H. Friend and F. C. Spano, Phys. Rev. Lett. **98**, 206406 (2007).
 - ¹⁸ C.-X. Sheng, M. Tong, S. Singh and Z. V. Vardeny, Phys. Rev. B **75**, 085206 (2007).
 - ¹⁹ S. Singh, T. Drori and Z.V. Vardeny, Phys. Rev. B **77**, 195304 (2008).
 - ²⁰ H. A. Mizes and E. M. Conwell, Phys. Rev. B **50** 11243 (1994).
 - ²¹ M. W. Wu and E. M. Conwell, Phys. Rev. B **56**, R10060 (1997).
 - ²² E. M. Conwell, Phys. Rev. B **57**, 14200 (1998).
 - ²³ H-F. Meng, Phys. Rev. B **58**, 3888 (1998).
 - ²⁴ A. Ruini, M. J. Caldas, G. Bussi and E. Molinari, Phys. Rev. Lett. **88**, 206403 (2002).
 - ²⁵ J. Cornil, D. A. dos Santos, X. Crispin, R. Silbey and J. L. Brédas, J. Am. Chem. Soc. **120**, 1289 (1998).
 - ²⁶ D. Beljonne, J. Cornil, R. Silbey, P. Millié and J. L. Brédas, J. Chem. Phys. **112**, 4749 (2000).
 - ²⁷ F. C. Spano, J. Chem. Phys. **122**, 234701 (2005).
 - ²⁸ W. Barford, J. Chem. Phys. **126**, 134905 (2007).
 - ²⁹ S. N. Dixit, D. Guo and S. Mazumdar, Phys. Rev. B **43**, 6781 (1991). D. Guo, S. Mazumdar, S. N. Dixit, F. Kajzar, F. Jarka, Y. Kawabe and N. Peyghambarian, Phys. Rev B **48**, 1433 (1993).
 - ³⁰ S. Abe, M. Schreiber, W.-P. Su and J. Yu, Phys. Rev. B **45**, 9432 (1992).
 - ³¹ M. Yu. Lavrentiev, W. Barford, S. J. Martin, H. Daly and R. J. Bursill, Phys. Rev. B **59**, 9987 (1999).
 - ³² D. Beljonne, J. Cornil, Z. Shuai, J. L. Brédas, F. Rohlffing, D. D. C. Bradley, W. E. Torruellas, V. Ricci, and G. I. Stegeman, Phys. Rev. B **55**, 1505 (1997).
 - ³³ A. Shukla, H. Ghosh and S. Mazumdar, Phys. Rev. B **67**, 245203 (2003).
 - ³⁴ G. Dicker, M. P. de Haas, L. D. A. Siebbeles, and J. M. Warman, Phys. Rev. B **70**, 045203 (2004).
 - ³⁵ E. Hendry, M. Koeberg, J. M. Schins, H. K. Nienhuys, V. Sunström, L. D. A. Siebbeles and M. Bonn, Phys. Rev. B **71**, 125201 (2005).
 - ³⁶ S. V. Frolov, Z. Bao, M. Wohlgenannt and Z. V. Vardeny, Phys. Rev. Lett. **85**, 2196 (2000).
 - ³⁷ S. V. Frolov, Z. Bao, M. Wohlgenannt and Z. V. Vardeny, Phys. Rev. B **65**, 205209 (2002).
 - ³⁸ M. Liess, S. Jeglinski, Z. V. Vardeny, M. Ozaki, K. Yoshino, Y. Ding and T. Barton, Phys. Rev. B **56**, 15712 (1997).
 - ³⁹ D. M. Basko and E. M. Conwell, Phys. Rev. B **66**, 155210 (2002)
 - ⁴⁰ P. B. Miranda, D. Moses and A. J. Heeger, Phys. Rev. B **64**, 081201 (R) (2001).
 - ⁴¹ M. A. Stevens, C. Silva, D. M. Russell, R. H. Friend, Phys. Rev. B **63**, 165213 (2001).
 - ⁴² Z. V. Vardeny, private communication.
 - ⁴³ R. Pariser and R. G. Parr, J. Chem. Phys. **21**, 466 (1953)
 - ⁴⁴ J. A. Pople, Trans. Faraday Soc. **49**, 1375 (1953).
 - ⁴⁵ M. Chandross and S. Mazumdar, Phys. Rev. B **55**, 1497 (1997).
 - ⁴⁶ M. Chandross, Y. Shimoi and S. Mazumdar, Phys. Rev. B **59**, 4822 (1999).
 - ⁴⁷ R. S. Mulliken, J. Am. Chem. Soc. **74**, 811 (1952).
 - ⁴⁸ R. Osterbacka, C. P. An, X. M. Jiang and Z. V. Vardeny, Science, **287**, 839 (2000).
 - ⁴⁹ Y. Zhang, Z. Wang, M.-K. Ng and L. J. Rothberg, J. Phys. Chem. B **111**, 13211 (2007).
 - ⁵⁰ H. Marciniak, M. Fiebig, M. Huth, S. Schiefer, B. Nickel, F. Selmaier and S. Lochbrunner, Phys. Rev. Lett. **99**, 176402 (2007).
 - ⁵¹ A. C. Morteani, P. Sreearunothai, L. M. Herz, R. H. Friend and C. Silva, Phys. Rev. Lett. **92**, 247402 (2004).
 - ⁵² P. Sreearunothai, A. C. Morteani, I. Avilov, J. Cornil, D. Beljonne, R. H. Friend, R. T. Phillips, C. Silva and L. M. Herz, Phys. Rev. Lett. **96**, 117403 (2006).
 - ⁵³ I.-W. Hwang, D. Moses and A. J. Heeger, J. Phys. Chem. C **112**, 4350 (2008).
 - ⁵⁴ T. Drori, C. X. Sheng, A. Ndobe, S. Singh, J. Holt, Z. V. Vardeny, Phys. Rev. Lett. **101**, 037401 (2008).
 - ⁵⁵ Z. Wang, H. Zhao and S. Mazumdar, Phys. Rev. B **74**, 195406 (2006).